Vibronic structure in the carbon 1*s* photoelectron spectra of HCCH and DCCD

K. J. Børve and L. J. Sæthre
Department of Chemistry, University of Bergen, N-5007 Bergen, Norway

T. D. Thomas
Department of Chemistry, Oregon State University, Corvallis, Oregon 97331-4003

T. X. Carroll
Keuka College, Keuka Park, New York 14478

N. Berrah
Physics Department, Western Michigan University, Kalamazoo, Michigan 49008

J. D. Bozek
Advanced Light Source, Lawrence Berkeley National Laboratory, University of California, Berkeley, California 94720

E. Kukk
Physics Department, Western Michigan University, Kalamazoo, Michigan 49008
and Advanced Light Source, Lawrence Berkeley National Laboratory, University of California, Berkeley, California 94720
(Received 17 July 2000; published 6 December 2000)

The carbon 1*s* photoelectron spectra of HCCH and DCCD have been measured at a photon energy of 330 eV and an instrumental resolution about half the natural linewidth. The vibrational structure in the spectra has been analyzed in terms of a model in which the parameters are the force constants for carbon-carbon and carbon-hydrogen stretching in the core-ionized molecules and the changes in bond lengths between the core-ionized and neutral molecules. Within this model, three different approaches to core-hole localization have been considered. Treating the core hole as completely localized, with the molecular motion following the diabatic energy surfaces, does not describe the data correctly. Treating the core hole as completely delocalized, with the molecular motion following the adiabatic surfaces, gives a good fit to the spectra but leads to zero-point energies that are completely unreasonable. A fit that takes into account vibronic coupling between the vibrational manifolds of the $^2\Sigma_u^+$ and $^2\Sigma_g^+$ electronic states of the ion gives good agreement with the data and leads to reasonable molecular parameters. *Ab initio* calculations of the molecular properties of the core-ionized molecule give results that are in excellent agreement with those obtained from this fit. The lifetime width for the carbon 1*s* hole state is 106 ± 2 meV, significantly higher than for CH_4 (95 ± 2 meV). This result is not in accord with predictions based on a one-center model of Auger decay.

DOI: 10.1103/PhysRevA.63.012506 PACS number(s): 33.60.Fy, 31.10.+z, 33.15.Mt, 33.20.Wr

I. INTRODUCTION

Inner-shell photoelectron spectra are characterized by several features of physical interest. These include the line position, reflecting the chemical environment of the atom from which the electron has been removed, the line shape, revealing the dynamics of the deexcitation of the core hole, vibronic structure, dependent on changes in equilibrium molecular geometry upon core ionization, and, in some cases, molecular-field splitting, providing insight into the asymmetry of the environment of the core hole. For symmetric molecules such as ethyne (acetylene), additional structure can appear in the spectrum; this arises from the splitting of the *gerade* and *ungerade* carbon 1*s* molecular orbitals. Understanding the vibronic structure plays a key role in the analysis of such spectra. On the one hand, the vibronic structure is of interest in its own right and provides an important test of theoretical models that predict molecular structure. On the other, the vibronic structure can obscure the other features of interest, especially if there are inequivalent atoms of the same element in the molecule, leading to overlapping spectra. As a result, there has been considerable interest in analyzing such vibronic structure and in developing models to predict and understand it.

A variety of approaches has been used to analyze vibronic structure in inner-shell photoelectron spectra. The simplest has been to fit a spectrum with a series of peaks, using positions and intensities as fitting parameters. A step beyond this is to use models, such as the harmonic-oscillator model or the linear-coupling model; in this case, the fits give fundamental vibrational frequencies and changes in normal coordinates. While such approaches are useful for diatomic molecules and such highly symmetric molecules as methane, they become less useful for more complicated molecules in which there might be contributions from several vibrational modes. In particular, for complex molecules, it may be difficult or impossible to derive molecular parameters (force constants and changes in bond lengths and bond angles) from the fitting parameters. A third approach has been to use *ab initio* theory to predict the vibronic structure and then to

compare the prediction with the experimental spectrum. If the agreement is good, then the parameters of interest can be taken from the theory. Here we explore a fourth approach, namely, to fit the vibronic structure with the force constants and bond-length changes as the adjustable parameters. Then the fitting procedure gives directly the molecular parameters of interest. Since the vibrational intensities and energies depend on the atomic masses, consideration of different isotopomers, for instance, HCCH and DCCD, helps to give a more complete picture. We believe that this is the first time that such an approach has been used for any but the simplest inner-shell photoelectron spectra.

Inner-shell ionization of molecules with equivalent atoms, such as ethyne, presents a particular set of theoretical problems. At the symmetry-restricted-molecular-orbital level of theory, a carbon 1*s* hole in ethyne is delocalized over the two carbon atoms. It was, however, recognized quite early that calculations based on such a starting point have to take extensive account of electron correlation in order to give correct core-ionization energies [1,2]. It was also recognized that a more efficient route to predicting core-ionization energies is obtained by allowing the hole to localize on one of the equivalent carbon atoms. In this case, the important effects of hole-electron correlation, which involve shrinkage of the atomic orbitals on the atom with the core hole and polarization of the valence molecular orbitals towards the core hole, are automatically included in the calculation. While this procedure is conceptually unsatisfactory in that it does not take into account the inherent symmetry of the molecule, little improvement in energies is obtained by combining localized-hole functions to give wave functions that display the full symmetry of the molecule [3].

For the vibrational structure in such molecules, the situation is quite different. In contrast to the case for core-ionization energies, predictions for the vibrational structure of the ionization spectrum based on potential-energy surfaces in the localized-hole model may be very different from those based on symmetry-projected wave functions. This difference can be understood from Fig. 1, which shows schematically the potential-energy curves for distortion of the geometry along a coordinate q that lifts the equivalence of two symmetry-related atoms. Figure 1(a) shows this for a localized hole, with left and right *diabatic* potential curves, one for each site of ionization. The corresponding potentials based on symmetry-projected wave functions must reflect the full symmetry of the molecule, and Figs. 1(b) and 1(c) show typical *adiabatic* potentials for the cases of weak and strong electronic coupling of the localized-hole states. The important parameter in determining the coupling is β, equal to $\langle \Psi_L | \hat{H} | \Psi_R \rangle$, where Ψ_L and Ψ_R are wave functions with the core hole localized on the left or right, and $\hat{H}$ is the Hamiltonian of the system. In these figures, β is reflected in the energy difference between the adiabatic potentials at the symmetry point, as 2β. The main point to be made is that the potential-energy curves in either Fig. 1(b) or 1(c) are quite different from those in Fig. 1(a), and so are the corresponding vibrational energy levels and Franck-Condon factors. For a number of symmetric molecules [4–8] it has been found

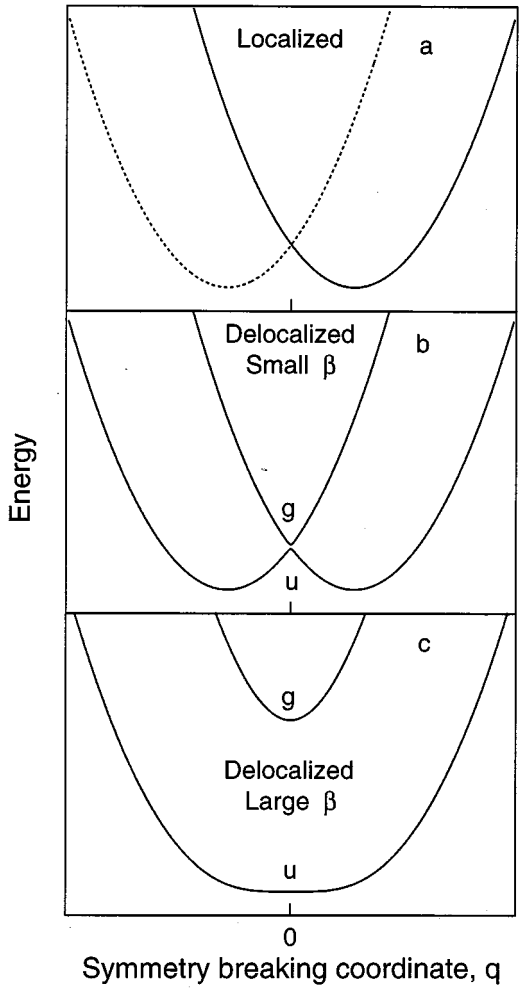

FIG. 1. Schematic representation of potential-energy curves for a symmetric molecule. (a) Diabatic curves. (b) Adiabatic curves derived from A for $\beta \approx 0$. (c) Adiabatic curves derived from A for large β.

that the vibronic structure is predicted well by a localized model, that is, by curves similar to those shown in Fig. 1(a). Taking carbon dioxide as an example, localization of the core hole on one of the oxygen atoms leads to a decrease in the length of the bond attached to the core-ionized oxygen and an elongation of the other bond. Such an asymmetry gives rise to excitation of the antisymmetric carbon-oxygen stretching mode in the core ionization of CO_2, as is indeed observed in the oxygen 1*s* photoelectron spectrum [6,8]. This result is contrary to what would be expected on the basis of the formally correct adiabatic potential-energy curves, which resemble those shown in Fig. 1(b); according to this picture excitation of the asymmetric stretching mode is symmetry forbidden. Similar symmetry breaking occurs in the core ionization of sulfur in CS_2 [4] and of carbon in CH_3CH_3 and CH_2CH_2 [5,7], for which the vibrational structure is well represented by a model in which it is assumed that the core hole is completely localized.

This excitation of apparently forbidden antisymmetric modes in such molecules as these was predicted by Domcke

and Cederbaum [9], who noted that if the splitting between the adiabatic potential curves, 2β, is very small, there will be strong coupling between the vibronic levels of the *gerade* and *ungerade* electronic states, and the motion will follow the diabatic curves rather than the adiabatic curves. Such strong vibronic coupling is the rule for the molecules that have been considered so far. For CS_2, CO_2, and CH_3CH_3, the distances between the equivalent atoms are relatively long and the electronic coupling between the core orbitals in the equivalent atoms is weak—2β is of the order of 1 meV or less. As a result, the photoelectron spectra for these molecules is well described in the localized approximation. Even for CH_2CH_2, with 2β equal to 20–50 meV, the vibrational structure appears to be reasonably well described by a localized, diabatic model [5,7]. A consideration of the adiabaticity of the motion by Thomas *et al.* [7] indicates that this is reasonable.

For ethyne, the ground state of the core-ionized molecule is far from degenerate; the splitting between the $1\sigma_u^{-1}(^2\Sigma_u^+)$ and $1\sigma_g^{-1}(^2\Sigma_g^+)$ states, 2β, is about 100 meV [10]. This large value makes the adiabatic potentials closer to those shown in Fig. 1(c) than to those of Fig. 1(b), and, as 2β is not negligible compared with the characteristic vibrational energy of the antisymmetric carbon-hydrogen stretching mode (408 meV in HCCH and 302 meV in DCCD) [11], it may put core-ionized ethyne near the borderline between diabatic and adiabatic behavior. These molecules thus present an interesting opportunity to investigate the effects of vibronic coupling in a situation that is intermediate between that found for the core ionization of CO_2 and CS_2 and that found for valence molecular orbitals, where the relevant splitting is very large and a delocalized picture certainly applies.

Here we report on measurements and analysis of the carbon 1*s* photoelectron spectra of HCCH and DCCD. The measurements have been made with a total instrumental resolution that is less than half the natural linewidth of the carbon 1*s* hole state. The analysis includes high-level *ab initio* calculations of the relevant potential-energy surfaces of the neutral and core-ionized molecules as well as a detailed consideration of methods to include the effects of vibronic coupling on the spectra. Our presentation is as follows. First we discuss the experimental methods and show the measured spectra. Then, in order to prepare for a full discussion of the vibronic structure in these spectra, we describe accurate theoretical calculations of the diabatic and adiabatic potential-energy surfaces for core-ionized ethyne. Third, these potentials are employed to develop a concise theory of vibronic coupling in the antisymmetric carbon-hydrogen stretching mode. Then, using the results of this theoretical analysis, three fitting models that are defined in terms of force constants and geometry parameters are applied to the experimental carbon 1*s* photoelectron spectra of HCCH and DCCD. The models include one in which the core hole is completely localized on one of the carbon atoms (with the molecular motion following the diabatic energy surfaces), one in which the core hole is treated as if it is completely delocalized between the two carbon atoms (with the motion following the adiabatic energy surfaces), and one that considers vibronic coupling between the $^2\Sigma_u^+$ and $^2\Sigma_g^+$ ionic states in detail. From the goodness of these fits and a comparison of the derived parameters with theory, the question of vibronic coupling in core-ionized ethyne is resolved. Finally, drawing on our best model of the vibronic structure, we discuss, on a broad basis, the carbon 1*s* spectrum of ethyne.

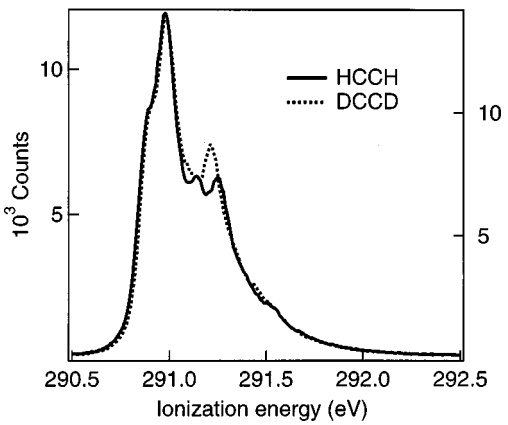

FIG. 2. Experimental carbon 1*s* photoelectron spectra of HCCH and DCCD measured at a photon energy of 330 eV.

II. EXPERIMENTAL PROCEDURE AND RESULTS

The experimental procedures are the same as those we have described in previous studies of carbon 1*s* photoelectron spectra [12–14]. Photons of 330 eV with a resolution of 32 meV were obtained from beamline 9.0.1 of the Advanced light source of the Lawrence Berkeley National Laboratory. The gas-phase photoelectron spectra of HCCH and DCCD were measured using a Scienta SES-200 electron spectrometer set for an electron-energy resolution of 28 meV [15]. The combined experimental resolution in the photoelectron spectra, including 15 meV for Doppler broadening, is 45 meV and is approximately Gaussian. The analyzer was set at an angle of 54.7° to the polarization direction of the photons and perpendicular to the propagation direction.

Although relative energies are known reasonably accurately, the absolute ionization energy scale is uncertain. We have chosen an energy scale such that the energy averaged over the vibrational profile corresponds to the value of 291.14 ± 0.05 eV for the vertical ionization energy obtained by Cavell [16] from x-ray photoelectron spectroscopy. This value is itself uncertain, since Tronc, King, and Read [17] give a value of 291.19 ± 0.03 eV for what is presumably the energy of the vibrational ground state of the $^2\Sigma_u^+$ electronic state. Since the vertical ionization energy should be higher than the adiabatic by the average vibrational excitation energy—about 0.17 eV—there is an unresolved discrepancy between these values. The results of the measurements for HCCH and DCCD are shown in Fig. 2. In describing these spectra, we adopt a notation appropriate to the adiabatic electronic states, $^2\Sigma_g^+$ and $^2\Sigma_u^+$. The principal peak, at about 291 eV in Fig. 2, arises from ionization to the lowest vibrational state of the $^2\Sigma_g^+$ electronic state. The shoulder at about 0.1 eV lower in ionization energy is then due to ionization to

TABLE I. Optimized geometry parameters (in Å) for neutral ethyne (HCCH) and ethyne with a localized carbon 1*s* hole (HCC*H$^+$).

	HCCH		HCC*H$^+$		
	R_{CC}	R_{CH}	R_{CC*}	R_{C*H}	R_{CH}
Experimental[a]	1.2033[a],1.2024[b]	1.0605[a],1.0625[b]			
MR-ACPF	1.2060	1.0625	1.1619	1.0371	1.0795
MR-ACPF[c]	1.2036	1.0615	1.1596	1.0371	1.0780

[a]Reference [18].
[b]Reference [19].
[c]Including estimates of core-valence electron correlation effects.

the corresponding vibrational state of the $^2\Sigma_u^+$ electronic state. The splitting between the $^2\Sigma_u^+$ and $^2\Sigma_g^+$ is also apparent in the structures on the high-ionization-energy side of the main peak. These arise primarily from the ionization to the $v=1$ state of the carbon-carbon stretching vibrational mode. The two spectra are very similar except at ionization energies of about 291.2 eV, where the DCCD spectrum shows a contribution from carbon-deuterium stretching; the corresponding contribution in HCCH is at higher-ionization energy and of lower intensity. Further discussion of the experimental results is found in Sec. VI, after we have developed the appropriate theoretical models for interpreting these spectra.

III. DIABATIC AND ADIABATIC MODELS OF THE VIBRATIONAL STRUCTURE

The ground state of most molecules, including that of ethyne, is well described within the Born-Oppenheimer approximation. This implies that the vibronic wave function may be factored into a vibrational wave function, χ and an electronic wave function, Φ, as indicated in Eq. (1):

$$\Psi_0(r,q)=\chi_0(q)\Phi_0(r;q). \tag{1}$$

In this expression, r represents the coordinates of the electrons and q describes the nuclear motion for the normal mode of interest. In this section, a similar assumption of separation of electronic and nuclear degrees of freedom is made for the core-ionized ethyne molecule; in Sec. IV we consider a more general case. If the electronic wave function is determined for a localized hole, we have a diabatic model. If, on the other hand, the electronic wave function is chosen to approximate a properly symmetry-adapted eigenfunction of the electronic Hamiltonian, we obtain an adiabatic model. In either case, focus will be on the associated potential-energy surfaces, in terms of the following coordinates: $q_c=R_{CC}$, $q_g=(R_L+R_R)/\sqrt{2}$, and $q_u=(R_L-R_R)/\sqrt{2}$, where R_{CC} denotes the carbon-carbon bond length and R_L and R_R denote the left and right carbon-hydrogen bond lengths, respectively. In these definitions, the subscripts u and g indicate the symmetry of the vibrational mode, with u referring to the antisymmetric carbon-hydrogen stretching mode and g to the symmetric modes. Since we do not expect the bending modes to be appreciably excited, we have not included these in our considerations.

The structures of neutral and core-ionized ethyne have been optimized at various levels of theory, using extensive atom-centered Gaussian basis sets. The details of the computations are covered in the Appendix; here it suffices to point out the qualitative difference between our two main computational methods for determining electronic wave functions: the multireference average coupled-pair functional method (MR-ACPF) and the restricted-active-space state interaction method (RASSI). MR-ACPF is a configuration-interaction method that is capable of providing a highly accurate description of the localized-hole state. The RASSI approach is valuable in that it allows for *ab initio* calculation of β, the electronic coupling integral between states with the hole localized on each of the two carbon atoms. In combination with the diabatic potential-energy surface, this allows for construction of an accurate potential also in the adiabatic approximation.

A. The diabatic potential-energy surface

The equilibrium geometry of core-ionized ethyne has been computed in the localized-hole approximation using MR-ACPF, and the results are summarized in Table I. Here we see that the bonds involving the ionized carbon (C*) are significantly shorter than those for the neutral molecule: as much as 4.4 pm in the case of the carbon-carbon bond and 2.4 pm for the bond to hydrogen. At the same time, the second carbon-hydrogen bond lengthens by 1.65 pm, indicating that changes in carbon-hydrogen bond lengths take place mainly along the antisymmetric stretching coordinate. Starting from the equilibrium geometry with the core-hole localized on the left carbon, we construct the potential-energy surface, V_L, for this ion. Because of the symmetry of the system, the diabatic surface for the core hole localized on the right carbon, V_R, is obtained easily as $V_R(\delta_c,\delta_g,q_u)=V_L(\delta_c,\delta_g,-q_u)$, where δ_c and δ_g denote displacements from this equilibrium geometry along the carbon-carbon and symmetric carbon-hydrogen stretching coordinates, respectively. Along the antisymmetric carbon-hydrogen stretching coordinate, the equilibrium geometry is found at $q_u=-q_0$, with $q_0=2.89$ pm. Within the harmonic approximation, the force field of this diabatic state may be parametrized as

TABLE II. Adiabatic geometry parameters (in Å) of core-ionized ethyne.

	$^2\Sigma_u^+$		$^2\Sigma_g^+$	
	R_{CC}	R_{CH}	R_{CC}	R_{CH}
MR-ACPF	1.1587	1.0579	1.1649	1.0580
MR-ACPF[a]	1.1564	1.0571	1.1626	1.0573

[a]Including estimates of core-valence electron correlation effects.

$$V_{L,2}(\delta_c,\delta_g,q_u)=\frac{1}{2}(\delta_c\,\delta_g\,q_u+q_0)\begin{pmatrix} f_c & f_{cg} & f_{cu} \\ f_{cg} & f_g & f_{gu} \\ f_{cu} & f_{gu} & f_u \end{pmatrix} \times\begin{pmatrix} \delta_c \\ \delta_g \\ q_u+q_0 \end{pmatrix}. \tag{2}$$

At the valence-correlated MR-ACPF level of theory, the force constants are determined in a cubic fit to be $f_c=19.83$, $f_{cg}=-0.21$, $f_g=6.35$, $f_{cu}=0.05$, $f_{gu}=0.49$, and $f_u=6.29$ aJ Å^{-2}. These correspond to harmonic frequencies of 2190, 3602, and 3316 cm^{-1} for the carbon-carbon and symmetric and antisymmetric carbon-hydrogen stretching modes, respectively. The accuracy of the procedure may be deduced from a corresponding calculation for neutral ethyne, which leads to harmonic frequencies of 2006, 3510, and 3422 cm^{-1}; these can be compared with values derived from experimental data of 2011, 3497, and 3415 cm^{-1}, respectively [18]. The respective fundamental frequencies are 1974, 3373, and 3289 cm^{-1} [11,19].

The force field may be improved by adding anharmonic terms, and from the fit just described, the dominating cubic terms are found to be

$$V_{L,3}(\delta_c,\delta_g,q_u)=f_{ccc}\delta_c^3+f_{ggg}\delta_g^3+f_{ggu}\delta_g^2(q_u+q_0)+f_{guu}\delta_g(q_u+q_0)^2 \tag{3}$$

with the following values of the cubic force constants (in units of aJ Å^{-3}): $f_{ccc}=-21.3$, $f_{ggg}=-4.5$, $f_{ggu}=-1.5$, and $f_{guu}=-13.4$.

B. The adiabatic potential-energy surface

Ab initio calculation of an accurate adiabatic potential surface for core-ionized ethyne presents a challenging problem in terms of electron correlation. A proper description of the electron-rich triple bond requires extensive electron correlation treatment in itself; in the core-ionized molecule, it is important to include in addition correlation between the hole and the valence electrons. In the present paper, accurate adiabatic energy surfaces are constructed by diagonalizing the electronic Hamiltonian in the basis of $\{\Phi_L,\Phi_R\}$, characterized by having the core hole localized on the *left* or the *right* carbon atom, respectively. This is advantageous for two reasons. First, it leads to expressions for the adiabatic potentials in terms of diabatic force constants, accessible to a variety of electronic structure methods, and, second, the resulting potential-energy surfaces are well suited for further analysis. The diagonal integrals are obtained in the MR-ACPF approximation as described in the preceding section, i.e., $H_{LL}=V_L$ and $H_{RR}=V_R$. The off-diagonal element, $H_{LR}=\beta$, is computed at the RASSI level of accuracy, after taking proper account of the very small, yet nonvanishing, electronic overlap integral $\langle\Phi_L|\Phi_R\rangle$.

The electronic-coupling integral β, which reflects the bonding/antibonding character of the 1σ molecular orbitals, is expected to depend strongly on the carbon-carbon distance, decreasing to zero at large distances, but is expected to depend only weakly on the carbon-hydrogen distance. Numerical calculations of β on the same grid as used for the force constants of the diabatic states verify these expectations. To a very good approximation,

$$\beta(\delta_c)=\beta_0+\beta_c\delta_c+\tfrac{1}{2}\beta_{cc}\delta_c^2, \tag{4}$$

where RASSI calculations gave values of 9.84×10^{-3} aJ ($=61.4$ meV), -6.13×10^{-2} aJ A^{-1}, and 0.49 aJ Å^{-2} for β_0, β_c, and β_{cc}, respectively. This dependence of β on the carbon-carbon bond length is reflected in the force constants and equilibrium bond lengths for the carbon-carbon bond, as discussed in the next paragraph.

Diagonalization of the 2 by 2 Hamiltonian gives the two adiabatic potentials; the geometric parameters obtained by this procedure are given on Table II. Neglecting anharmonic coupling between modes of different parity, we may discuss the *gerade* and *ungerade* vibrational modes associated with these potentials separately. We start out by first considering the *gerade* stretching modes, for which the adiabatic potential surfaces may be written in terms of the *left* diabatic potential as

$$V_\pm(\delta_c,\delta_g)=V_L(\delta_c,\delta_g,0)\pm\beta(\delta_c). \tag{5}$$

An inspection of the wave functions shows that the higher-energy state is of $^2\Sigma_g^+$ symmetry, and, in the equations to come, quantities pertaining to $^2\Sigma_g^+$ are obtained by choosing the upper sign and those pertaining to the $^2\Sigma_u^+$ state are obtained by choosing the lower sign.

Relative to the diabatic equilibrium geometry, the stationary points on the adiabatic surfaces are given by $q_u=0$, $\delta_{c\pm}\approx\mp\beta_c/f_c$ and $\delta_{g\pm}\approx-(f_{gu}q_0+f_{guu}q_0^2+f_{cg}\delta_{c\pm})/f_g$. As noted above, β_c is negative, since the coupling integral β decreases with increasing carbon-carbon distance. As a consequence, these equations imply that the $^2\Sigma_g^+$ state has a slightly longer carbon-carbon bond than does the lower state; from the computed force constants, the difference is 0.6 pm. On the other hand, the shift in average carbon-hydrogen bond length is approximately the same in both adiabatic states, with only a very small difference introduced through the f_{cg} coupling constant. Similar results are seen for the force constants. The harmonic force constants for the *gerade* carbon-hydrogen stretch change only minutely from their diabatic values. However, the two adiabatic states may differ appreciably in terms of the carbon-carbon stretching frequency, since the corresponding force constants are given by

$f_{c\pm} \approx f_c + 6 f_{ccc} \delta_{c\pm} \pm \beta_{cc}$. The second and third terms of this expression are intrinsically of opposite sign, and, for the case considered here, are calculated to be of comparable magnitude. For harmonic diabatic potentials (i.e., $f_{ccc}=0$), the difference between the two force constants amounts to twice β_{cc}, or close to 1 aJ Å^{-2}. With anharmonicity taken into account, this difference reduces to 0.2 aJ Å^{-2}. In the analysis of the experimental data, discussed in Sec. VI, we will see that these effects are apparent in the photoelectron spectra.

In the direction of the antisymmetric carbon-hydrogen stretching coordinate (that is, the *ungerade* vibrational mode) the potential-energy curves of the two adiabatic states are given by

$$V_{\pm}(q_u) = 1/2[V_L(\delta_{c\pm}, \delta_{g\pm}, q_u) + V_L(\delta_{c\pm}, \delta_{g\pm}, -q_u)] \pm \sqrt{1/4[V_L(\delta_{c\pm}, \delta_{g\pm}, q_u) - V_L(\delta_{c\pm}, \delta_{g\pm}, -q_u)]^2 + \beta(\delta_{c\pm})^2}. \tag{6}$$

Depending on the relative magnitude of the coupling integral and the slope of the diabatic potential at $q_u=0$, the lower adiabatic surface shows either a single-well [Fig. 1(c)] or a double-well potential [Fig. 1(b)]. For ethyne, the former situation applies and is the only case considered in detail. As has been tacitly assumed in the preceding paragraph, the resulting equilibrium geometries are found at $q_u=0$, and the adiabatic force constants are given by

$$f_{u\pm} = f_u \pm \frac{1}{|\beta(\delta_{c\pm})|} \left(\frac{\partial V_L}{\partial q_u} \right)^2_{(\delta_{c\pm}, \delta_{g\pm}, 0)}. \tag{7}$$

From the computed values for the diabatic force constants and coupling parameters, this expression gives a low force constant of 3.0 aJ Å^{-2} for the $^2\Sigma_u^+$ state, and a correspondingly high value of 9.6 aJ Å^{-2} for the upper adiabatic state, $^2\Sigma_g^+$, in qualitative agreement with the curves shown in Fig. 1(c).

IV. VIBRONIC-COUPLING MODEL OF THE VIBRATIONAL STRUCTURE

For the carbon-carbon and symmetric carbon-hydrogen stretching modes, the differences between a diabatic and an adiabatic picture are small and, as noted above, are reflected in small differences in bond lengths and force constants between the two approaches. Furthermore, the adiabatic electronic wave functions display only a weak dependence on the corresponding nuclear coordinates, making vibronic coupling unimportant for these modes. By contrast, in the direction of the antisymmetric C-H stretching coordinate, the diabatic and adiabatic potential curves are very different. Therefore, in order to make quantitative predictions for the contribution from the antisymmetric carbon-hydrogen stretching mode to the vibrational structure, it is necessary to develop models that take vibronic coupling explicitly into account. A framework for such models has been given by Köppel, Domcke, and Cederbaum [20] and we use their approach as a basis for our description. Only the antisymmetric carbon-hydrogen stretching mode is considered explicitly, and for simplicity, the subscript is dropped from the coordinate q_u.

The nonrelativistic molecular Hamiltonian may be written in terms of the nuclear kinetic-energy operator and the electronic Hamiltonian as

$$\hat{H} = \hat{T}_N + \hat{H}_e. \tag{8}$$

The nuclear kinetic operator is $\hat{T}_N = -\alpha \partial^2/\partial q^2$, where the constant $\alpha = \hbar^2/2\mu$ is defined in terms of the reduced mass of a carbon-hydrogen unit. In the presence of near degeneracy in the electronic spectrum, a more general *ansatz* than given in Eq. (1) is often required for the vibronic wave function. This is the case for the two lowest states of core-ionized ethyne, where, following Köppel, Domcke, and Cederbaum [20], Eq. (9) defines our starting point:

$$\Psi(r,q) = \chi_1(q)\Phi_1(r;q) + \chi_2(q)\Phi_2(r;q). \tag{9}$$

Here, as before, χ represents a vibrational wave function and Φ an electronic function. Insertion of Eq. (9) into the Schrödinger equation defined by Eq. (8), followed by projection onto each of the two orthonormal electronic states, leads to

$$0 = \langle \Phi_1 | \hat{H} - E | \Psi \rangle = (\hat{T}_N + V_1 - \hat{\Lambda}_{11} - E)\chi_1 + (V_{12} - \hat{\Lambda}_{12})\chi_2, \tag{10}$$

$$0 = \langle \Phi_2 | \hat{H} - E | \Psi \rangle = (V_{21} - \hat{\Lambda}_{21})\chi_1 + (\hat{T}_N + V_2 - \hat{\Lambda}_{22} - E)\chi_2. \tag{11}$$

In Eqs. (10) and (11), operators acting on the nuclear degrees of freedom have been introduced:

$$V_n = \langle \Phi_n | \hat{H}_e | \Phi_n \rangle, \quad V_{nm} = \langle \Phi_n | \hat{H}_e | \Phi_m \rangle, \quad n \neq m, \tag{12}$$

$$\hat{\Lambda}_{nm} = -\langle \Phi_n | \hat{T}_N | \Phi_m \rangle + 2\alpha \langle \Phi_n | \partial/\partial q | \Phi_m \rangle \partial/\partial q. \tag{13}$$

In the following, Eqs. (10) and (11) are discussed within two different representations of the electronic states, commonly referred to as diabatic and adiabatic bases.

A. Localized core-hole states—diabatic potentials

In the localized, or diabatic, representation, the core-hole wave functions change only slowly with the nuclear coordinates, and to a good approximation one may write

$$\partial\Phi_L/\partial q \approx \partial\Phi_R/\partial q \approx 0. \tag{14}$$

Equation (14) ensures $\hat{\Lambda}=0$. However, these electronic wave functions are not proper eigenstates of the electronic Hamiltonian, implying a nonzero value of $V_{LR}(=\beta)$.

The *diabatic approximation* results from neglecting V_{LR} altogether. Because of the symmetry in the problem, the diabatic potentials are related through inversion as $\hat{i}V_L=V_R$. Within the harmonic approximation, $V_R=f(q-q_0)^2/2$ and $V_L=f(q+q_0)^2/2$ for positive q_0. The vibrational spectra (ε_v, $v=0,1,\ldots$) are the same for the left and right diabatic potentials.

The effects of *vibronic coupling* may be examined by solving Eqs. (10) and (11) while retaining a nonzero electronic coupling integral $V_{LR}=\beta$. To proceed, relative phase factors are chosen such that the left and right electronic wave functions transform into one another under inversion, and the same choice is made for pairs of corresponding vibrational eigenstates:

$$\hat{i}|v_L\rangle=|v_R\rangle. \tag{15}$$

It may be noted that for the present system of core-ionized ethyne, these definitions make $\beta\geqslant 0$. The overall vibronic wave function, Eq. (9), must reflect the full symmetry of the molecule, and this implies that the nuclear functions appearing in Eqs. (10)–(11) must display either *ungerade* or *gerade* character: $\hat{i}\chi_L=\pm\chi_R$. Expanding these χ functions in the set of vibrational functions for the diabatic states ($|v_L\rangle$ and $|v_R\rangle$) while Eq. (15), transforms Eq. (10) into the following set of equations:

$$\sum_{v=0}[(\varepsilon_v-E)|v_L\rangle\pm\beta|v_R\rangle]c_v=0 \tag{16}$$

and a corresponding set with the left and right indices exchanged. In this expression the ε_v's are the vibrational energies of the diabatic potentials. In the limit that $\beta=0$, we have the degenerate case, treated by Domcke and Cederbaum [9]. In this case, the energy levels, vibrational wave functions, and Franck-Condon factors are those appropriate for the diabatic potentials.

We now consider the effect of a nonzero value of β. At the MR-ACPF level of theory and neglecting coupling to other degrees of freedom, the diabatic potentials have a harmonic frequency of $\omega=420$ meV, and an equilibrium geometry of $q_0=0.0289$ Å. The electronic coupling integral is found to be essentially independent of q, at $\beta=61.4$ meV. This allows us to transform Eq. (16) into a set of algebraic equations by projecting onto the set of vibrational eigenstates of the *left* potential,

$$(\varepsilon_v-E)c_v\pm\beta\sum_{v'=0}\langle v_L|v'_R\rangle c_{v'}=0. \tag{17}$$

Selecting the plus sign in front of β in Eq. (17) leads to solutions of overall *gerade* symmetry, whereas the minus sign gives the *ungerade* solutions. The expansion converges very fast, and the essential features of the vibronic coupling in ethyne are recovered with only two vibrational states for each diabatic potential. Use of the experimental *ungerade/gerade* intensity ratio, leads to the following intensity ratio between the four lowest vibronic states in core-ionized HCCH: 1:1.3:0.1:0.02.

It is useful to consider Eq. (17) in the limit of small overlap between the right-hand and left-hand functions. In this case, we need be concerned only with the overlap integrals $\langle v_L|v_R\rangle$, where the left and right-hand vibrational functions have the same quantum number. The energy levels are then given by the expression

$$E=\varepsilon_v\pm\beta\langle v_L|v_R\rangle. \tag{18}$$

From this, two features emerge. First the diabatic limit is reached when either β is very small (as discussed above) or when the vibrational overlap is small, that is when q_0 is large. Second, we see that the apparent *u-g* splitting is equal to $2\beta\langle v_L|v_R\rangle$, and is, hence, dependent on both the vibrational state and the value of q_0 (which determines the vibrational overlap integral). Numerical evaluation of the energies shows that this approximation is reasonably good over a wide range of values of β and q_0.

B. Symmetry-adapted core-hole states

An alternate theoretical approach is to use the localized hole-state functions to construct proper eigenfunctions of the electronic Hamiltonian, as discussed in the context of adiabatic potential energy surfaces. At $q=0$, the resulting eigenfunctions transform according to the irreducible representations Σ_u and Σ_g, and by continuation, this labeling may be used at any q. Hence, in the following, the electronic wave functions and their associated nuclear functions are indexed by u and g, respectively, rather than ''+'' and ''−'' as during the discussion of adiabatic potentials.

By way of construction, $V_{ug}=V_{gu}=0$, and the relationship between localized and symmetry-adapted core-hole wave functions is

$$\begin{pmatrix}\Phi_u\\ \Phi_g\end{pmatrix}=\begin{pmatrix}\cos a(q) & \sin a(q)\\ -\sin a(q) & \cos a(q)\end{pmatrix}\begin{pmatrix}\Phi_L\\ \Phi_R\end{pmatrix}. \tag{19}$$

$a(q)$ passes from 0 to $-\pi/2$ as q goes from $-\infty$ to ∞, and varies rapidly near $q=0$. It may in general be computed from

$$a(q)=-\frac{1}{2}\tan^{-1}\left[\frac{2\beta}{V_R(q)-V_L(q)}\right],\quad q\leqslant 0$$

$$\wedge\ a(q)=-\frac{\pi}{2}-a(-q),\quad q>0. \tag{20}$$

Using Eqs. (13) and (19), one finds

$$\hat{\Lambda}_{uu}=\hat{\Lambda}_{gg}=-\alpha[a'(q)]^2, \tag{21}$$

$$\hat{\Lambda}_{ug}=-\alpha a''(q)-2\alpha a'(q)\partial/\partial q=-\hat{\Lambda}_{gu}. \tag{22}$$

The *adiabatic approximation* results from neglecting the $\hat{\Lambda}$ operator altogether, which is appropriate when $a'(q)$ is

small. In the limit of constant β and harmonic diabatic potentials, $|a'(0)| = f_u q_0/2\beta \equiv \eta$, and this condition results when either β is very large or the product $f_u q_0$ is very small. The *diabatic approximation* is valid at the other extreme, at very large η, i.e., when either β is very small or q_0 is very large, as we have seen in the discussion of the diabatic basis.

Finally, if $\hat{\Lambda}$ is retained as given in Eqs. (21)–(22), solving Eqs. (10)–(11) in the adiabatic basis gives the same result as when solving the vibronic problem in the diabatic basis. From a computational point of view, the diabatic basis is preferred because it leads to simpler matrix elements and a more rapidly converging expansion in terms of harmonic-oscillator functions. However, as we will see below, the adiabatic approach provides a simple way to understand the vibrational excitation pattern for the antisymmetric carbon-hydrogen stretching mode.

V. FITTING MODELS AND MOLECULAR PARAMETERS

A. Fitting procedures common for the various models

The experimental carbon 1*s* photoelectron spectra of HCCH and DCCD have been fit by modeling the vibrational structure with a set of force constants and changes in the bond lengths; the details of this procedure are discussed below. The advantage of using parameters that are directly related to the underlying potential-energy surface, rather than vibrational frequencies, is that a single set of parameters apply to all isotopomers of a molecule. The HCCH and DCCD spectra are fit simultaneously to a common set of these parameters as well as to the intrinsic linewidth, the $^2\Sigma_g - ^2\Sigma_u$ splitting, and the *ungerade/gerade* intensity ratio, with only a constant background, the overall height, and the overall position being separately adjustable for the two different isotopomers.

The shape of an individual line in the spectrum is modeled using the theory of post-collision interaction described by van der Straten, Morgenstern, and Niehaus [21]. This takes into account the interaction of the photoelectron with the high-energy Auger electron emitted in the deexcitation of the core-ionized molecule.

The Franck-Condon factors for the carbon-carbon stretching mode and for the symmetric carbon-hydrogen stretching mode are calculated from the changes in bond lengths and the force constants using the harmonic-oscillator model. For the antisymmetric carbon-hydrogen stretching mode the Franck-Condon factors are calculated either in the same way or from the explicit results of a vibronic-coupling model, as appropriate. Our experience has shown that the harmonic model overestimates the population of the higher vibrational states but that inclusion of anharmonic corrections leads to good agreement between observed and calculated intensities [13,22]. In the present case, we do not have sufficient information on the anharmonicities to make these corrections and have, therefore, used the harmonic model exclusively. This restriction leads to problems with the fitting procedure. The spectrum is dominated by the carbon-carbon stretching mode and the harmonic model predicts too much intensity for the $v=2$ and $v=3$ transitions. To compensate for this and to produce a better fit at high-ionization energies, the fitting procedure adjusts the parameters of the carbon-hydrogen stretching modes, which become meaningless. To minimize this problem, we have restricted the range of the fits to energies below that of the $v=2$ peak of the carbon-carbon stretching mode. This limit is indicated by the arrows in Fig. 3, which shows the data (points) as well as a fit to the data (lines); the fit is discussed in more detail below. It might appear that fitting over this restricted range would provide little information on the carbon-hydrogen stretching modes. However, the so-called carbon-carbon stretching mode does not involve only the carbon-carbon bond but also the carbon-hydrogen bonds. As a result, both the frequency and the Franck-Condon factors for this mode depend on the carbon-hydrogen force constant and the change in carbon-hydrogen bond length, and, furthermore, this dependence is not the same for DCCD as it is for HCCH. Consequently, fitting the position and intensity of the $v=1$ carbon-carbon stretching peak simultaneously in the two molecules provides information on the carbon-hydrogen parameters as well as on the carbon-carbon parameters. Additional information on carbon-hydrogen stretching is contained in the DCCD spectrum, where carbon-deuterium stretching modes make a major contribution to the peak at an ionization energy of 291.23 eV.

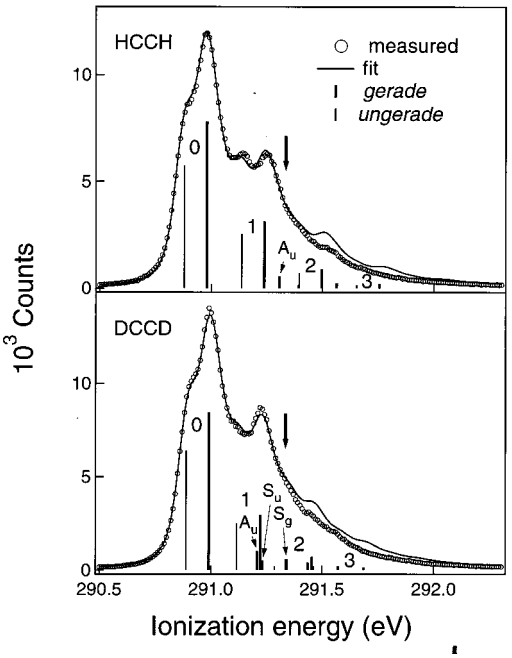

FIG. 3. Comparison of fits (lines) based on vibronic-coupling model with the experimental carbon 1*s* photoelectron spectra (circles) of HCCH and DCCD. The arrows show the upper limit of the data that were used for the fits. The notation *gerade* and *ungerade* refers to the total symmetry of the ionic state. The major vibronic transitions are identified as follows. The numbers 0, 1, 2, and 3 identify the members of the two carbon-carbon stretching progressions. The symbol A_u refers to a transition to a state that can be identified primarily as the $v=1$ member of the antisymmetric carbon-hydrogen stretching mode built on the $^2\Sigma_u^+$ electronic state. The symbols S_u and S_g indicate the $v=1$ members of the symmetric carbon-hydrogen stretching progressions.

TABLE III. Parameters derived from fitting the HCCH and DCCD photoelectron spectra with three different models and from theory. See the text for definitions of parameters.

	Localized (diabatic)		Delocalized (adiabatic)		Vibronic coupling	
	Fit	Theory	Fit	Theory	Fit	Theory
$^2\Sigma_g - {}^2\Sigma_u$ splitting[a] (meV)	101	0	102	123[b]	101.6	113[c]
Ungerade/gerade intensity ratio[d]	0.72		0.87		0.726	
	Force constant (aJ Å^{-2})					
$f_{c,g}$	19.1	19.8	18.2	20.0	18.6	20.0
$f_{c,u}$	17.4		17.3	19.8	17.5	19.8
f_g	6.2	6.3[e]	6.6	6.3	6.3	6.3
f_{u-}			1.8	3.0		
f_{u+}			11.5	9.6		
	Bond-length changes (pm)					
$\delta_{c,g}$	−4.4	−4.4	−4.4	−4.1	−4.36	−4.4
$\delta_{c,u}$	−4.4		−4.6	−4.7	−4.65	−4.4
δ_g	−1.9	−0.5	−0.8	−0.5	−0.8	−0.5
q_0	2.8	2.9			2.9	2.9

[a]Splitting between the $^2\Sigma_u(v=0)$ and $^2\Sigma_g(v=0)$ energies.
[b]Zero-point energies not included.
[c]Based on a harmonic diabatic potential with frequency $\omega = 411$ meV.
[d]Intensity to ionic states with overall *ungerade* intensity divided by intensity with *gerade* intensity.
[e]Average of force constants for the CH bond (5.8) and the C*H bond (6.8).

B. Diabatic model

The simplest model is the one that has been successfully applied to such molecules as CO_2, CS_2, and CH_3CH_3, namely, a completely localized hole [4,6,7]. This will be valid in the case where β is zero, as is the case for these molecules, or when q_0 is large. In such a case, there will be no u-g splitting apparent in the spectrum, since the product $\beta\langle v_L|v_R\rangle$ is very small. However, the u-g splitting is an important feature of the ethyne spectra, and it is apparent, therefore, that a localized model is unsuitable for our situation. We can make an *ad hoc* correction to this model by fitting with two spectra shifted by the $^2\Sigma_u - {}^2\Sigma_g$ energy difference, which is one of the fitting parameters. In this case, the molecular fitting parameters are the harmonic force constants for carbon-hydrogen and carbon-carbon stretching (f_g and f_c) and the changes in coordinates, δ_c, δ_g, and q_0. In keeping with the theoretical analysis, which indicates that the carbon-carbon force constants and bond-length changes depend on whether we are dealing with the $^2\Sigma_u$ or the $^2\Sigma_g$ state, there are two independent parameters for each of these: $f_{c,u}$, $f_{c,g}$, $\delta_{c,g}$, and $\delta_{c,u}$. The other fitting parameters are described in the first paragraph of this section. The calculation of line positions and intensities is done entirely within the harmonic-oscillator approximation. This approach gives a reasonably good fit to the data, with a value of χ^2 of 2.3. It is, however, difficult to justify this *ad hoc* treatment, and its apparent success is probably due to the fact that the spectrum is dominated by carbon-carbon stretching. As we have seen in the theoretical discussion, this excitation does not depend much on whether we use a diabatic or an adiabatic approach. Parameters of interest that have been derived from this fit are summarized in Table III.

C. Adiabatic model

At the other extreme is the adiabatic model, valid when η is large (that is, either β large or $f_u q_0$ small). As above, two states, $^2\Sigma_u$ and $^2\Sigma_g$, are assigned independent force constants for carbon-carbon stretching and independent values of δ_c. On the other hand, both states are described by a single force constant, f_g, for the symmetric carbon-hydrogen stretching mode and by a single change in average carbon-hydrogen bond length, δ_g. For the antisymmetric stretching mode the change in the normal coordinate is zero. Because of the symmetry of the vibrational wave functions, there will be no excitation of states of the antisymmetric carbon-hydrogen stretching mode with odd quantum numbers, and excitation of the even states only to the extent that the potentials of the core-ionized state differ in curvature from that of the unionized state. Since, to a fair approximation, the average of the antisymmetric carbon-hydrogen force constants for $^2\Sigma_u$ and $^2\Sigma_g$ is equal to the symmetric carbon-hydrogen force constant, a single additional parameter suffices to describe the antisymmetric stretching mode. Hence, four force constants and three bond-length changes are used to model vibrational energies and Franck-Condon factors for all significant final states in both HCCH and DCCD. Altogether 15 parameters have been determined in a least-squares fit to the HCCH and DCCD spectra, taken simultaneously.

A fit based on the adiabatic model is quite good, with $\chi^2 = 1.6$. The significant parameters are summarized in the column of Table III labeled ''delocalized, adiabatic,'' with frequencies derived from these parameters given in Table IV. Here, it suffices to point out that these parameters agree well with our theoretically computed numbers. In particular, the derived parameters for the antisymmetric carbon-hydrogen

TABLE IV. Vibrational frequencies derived from the fits to the HCCH and DCCD spectra (meV).

		Delocalized (adiabatic)			Vibronic coupling		
		CC[a]	CH sym.[b]	CH anti.[c]	CC[a]	CH sym.[b]	CH anti.[c]
HCCH	$^2\Sigma_g$	263	443	569	265	431	419[d]
	$^2\Sigma_u$	258	442	223	258	430	
DCCD	$^2\Sigma_g$	233	354	417	232	349	308[d]
	$^2\Sigma_u$	229	351	164	228	344	

[a]Carbon-carbon stretching.

[b]Symmetric carbon-hydrogen stretching.

[c]Antisymmetric carbon-hydrogen stretching.

[d]In the vibronic-coupling model, the states that involve antisymmetric carbon-hydrogen stretching are mixtures of $^2\Sigma_g$ and $^2\Sigma_u$ states.

stretching force constants are in accord with the theoretical prediction that one is much larger and one much smaller than the force constant for the symmetric stretching mode. This difference has important consequences with respect to the zero-point energy, which we consider next.

In this model of the spectra, the experimentally observed splitting between $^2\Sigma_g$ and $^2\Sigma_u$, determined to 102 meV, contains two contributions, an electronic term 2β, and a vibrational term, corresponding to the difference in zero-point energies between $^2\Sigma_g$ and $^2\Sigma_u$. It is to be noted that the experimental value of this splitting is the same for DCCD as for HCCH. As indicated in Sec. III, the theoretical value of the electronic contribution 2β, given by the hole-state calculations, is 123 meV. The zero-point contributions to the difference are readily calculated from the frequencies given in Table IV. They are, for the $^2\Sigma_g - ^2\Sigma_u$ difference, 176 meV for HCCH and 130 meV for DCCD. Both of these values are larger than the observed splitting, 102 meV, even without considering the additional contribution from the electronic-energy difference. Moreover, there is a significant difference, 46 meV, between the zero-point energy for HCCH and that for DCCD, although no such difference is observed experimentally.

Although the fit based on the delocalized model agrees well with the data, it is apparent that the parameters derived from this model are not reasonable, and that we must reject the model. The problem with the zero-point energy is intrinsic in the model; the zero-point energy for $^2\Sigma_g$ must be greater than that for $^2\Sigma_u$ because the curvature of the potential at the minimum is always greater for the former than for the latter. We will see below, after considering a vibronic-coupling model, why the fit is as good as it is.

D. Vibronic-coupling fitting model

In addition to the problems just mentioned, the diabatic and adiabatic fitting models suffer from an additional drawback. In these models, the splitting between the $^2\Sigma_g$ and $^2\Sigma_u$ is treated as a parameter that is independent of the other molecular parameters. That this is not the case can be seen from Eq. (18), where we see that the apparent splitting depends on both the electronic coupling integral and the vibrational overlap integral. The former depends on the carbon-carbon bond length and the latter on both this length and on the vibrational frequencies. A proper fitting procedure must take this coupling into account. We now consider a model that includes this feature as well as the effects of coupling between the $^2\Sigma_g$ and $^2\Sigma_u$ vibronic manifolds.

First, we note an important qualitative prediction of the vibronic-coupling theory for the antisymmetric carbon-hydrogen stretching mode. Referring to each vibronic level of this mode by its main adiabatic constituent, the Franck-Condon intensity for population of the $v=0$ state of the $^2\Sigma_u$ electronic state is very close to 1; that for the $v=1$ state of the $^2\Sigma_g$ electronic state, which also has overall *ungerade* symmetry, is close to zero. For the $v=0$ state of the $^2\Sigma_g$ electronic state the calculated intensity is less than 1, and, correspondingly the population of the $v=1$ state of the $^2\Sigma_u$ electronic state, which has overall *gerade* symmetry, has nonzero intensity. Thus, only three states receive significant intensity, the two $v=0$ states and the $v=1$ state of the $^2\Sigma_u$ electronic state.

While these intensities are most easily calculated using the diabatic basis, this intensity pattern is most easily understood in the adiabatic basis. In the limit of adiabatic behavior and in the limit that the vibrational potentials for the antisymmetric stretching are the same for the ionized state as for the ground state, only the $v=0$ states will be populated. However, because the characteristic vibrational spacing, about 400 meV, is not greatly different from the splitting between the $^2\Sigma_g$ and $^2\Sigma_u$ electronic states, about 100 meV, there is coupling (that is, vibronic coupling) between the $v=1$ state of $^2\Sigma_u$ and the $v=0$ state of $^2\Sigma_g$. Thus, the $v=1$ state of $^2\Sigma_u$ gains its intensity from the $v=0$ state of $^2\Sigma_g$. Similar coupling between $v=0$, $^2\Sigma_u$, and $v=1$; $^2\Sigma_g$, is, however, weak, because the corresponding energy difference is the *sum* of the vibrational energy and the $^2\Sigma_g - ^2\Sigma_u$ energy difference.

The free parameters in the vibronic fitting model are as follows. Six parameters describe the *gerade* vibrational motion; these are $f_{c,u}$, $f_{c,g}$, f_g, $\delta_{c,g}$, $\delta_{c,u}$, and δ_g, as previously described. Six parameters describe the background, overall intensity, and overall position in each of the two spectra. One parameter is Γ, the linewidth characteristic of the core-hole lifetime, and another is the *ungerade/gerade*

intensity ratio. Specifically, the latter is the ratio of total intensity involving final ionic states with overall *ungerade* symmetry to the intensity involving states with *gerade* symmetry. Three other parameters are β, q_0, and the $^2\Sigma_g - ^2\Sigma_u$ energy difference for the $v=0$ states. These three are not independent; β and q_0 are constrained to values that are consistent with the $^2\Sigma_g - ^2\Sigma_u$ energy difference. Thus, there are 16 independent parameters for the fit. In the fitting procedure, the Franck-Condon intensities for the *gerade* vibrational modes are calculated using the harmonic-oscillator approximation; those for the *ungerade* mode are calculated from β and q_0 using the vibronic-coupling model. As noted above, only the $v=0$ and $v=1$ states of this mode receive significant population.

A fit based on a vibronic-coupling model for the vibrational profile is shown in Fig. 3. Here the solid lines represent the fit and the open circles the data. Also shown in this figure are vertical lines to indicate the positions and intensities of the most important vibrational states that contribute to the spectrum. Over the range for which it has been made, the fit is good; the value of χ^2 is 1.5, somewhat better than obtained with either of the other models. At ionization energies above the cutoff, the fit deviates from the data in a manner consistent with that expected from the failure to include anharmonicity. The value of β derived from the fit is 57 meV, in good agreement with the value of 61.4 meV from *ab initio* theory. Other parameters derived from this fit are summarized in Table III and are discussed in detail in Sec. VI. Frequencies derived from these parameters are listed in Table IV.

E. Discussion of the fits

From the previous analysis, we see that neither an extreme localized, diabatic, model nor an extreme adiabatic model can account for the part of the vibrational structure that is due to the antisymmetric carbon-hydrogen stretching excitation. The first fails because it cannot produce the observed $^2\Sigma_g - ^2\Sigma_u$ energy difference, and the second fails because it leads to zero-point energies that are unreasonable. In spite of this failure, however, the adiabatic model can be made to give a good description of the spectrum by treating the $^2\Sigma_g - ^2\Sigma_u$ splitting as an independent parameter. The reason for this apparent success is that the least-squares fitting routine adjusts the force constants so that the $v=2$ vibrational of the $^2\Sigma_u$ electronic state corresponds with what is actually the $v=1$ state [23]. Thus, this model can artificially adjust itself to reproduce the data, but ultimately produces a physically unreasonable picture.

A good and physically reasonable description of the contribution of antisymmetric carbon-hydrogen stretching to the carbon 1*s* photoelectron spectra of ethyne can be obtained only if we explicitly take into account vibronic coupling between the *gerade* and *ungerade* electronic states. It is to be noted that the effect of this coupling extends beyond the relatively small structures in the spectra that can be attributed to this vibrational mode; the $^2\Sigma_g - ^2\Sigma_u$ energy splitting, which is a major feature of the spectrum, depends on this coupling. The other dominant features of the spectra arise from carbon-carbon stretching, and are only weakly influenced by vibronic coupling. This is apparent from Tables III and IV, where it is seen that the carbon-carbon force constants, bond-length changes, and stretching frequencies are essentially independent of whether we use the diabatic, adiabatic model, or vibronic-coupling model to fit the spectrum. Furthermore, these derived parameters are in good agreement with those predicted by *ab initio* theory.

VI. EXPERIMENTAL RESULTS AND DISCUSSION

The various parameters derived from the fits are bond-length changes, force constants, the intrinsic linewidth, the ungerade/gerade intensity ratio, and the $^2\Sigma_g - ^2\Sigma_u$ ($v=0$) energy difference. With a few exceptions, most of the derived parameters are rather independent of the fitting model. This result is not surprising, in that the spectra are dominated by contributions from the carbon-carbon stretching mode, which are not significantly affected by vibronic coupling. We discuss these results in detail below.

A. Bond-length changes and force constants

The most obvious feature of these results is that a decrease in equilibrium carbon-carbon bond length of about 4.5 pm accompanies core ionization. This shrinkage is a commonly observed feature for carbon-carbon and carbon-hydrogen bonds when carbon is core ionized, and presumably arises because of the collapse of the valence electrons towards the core when an inner-shell electron is removed. This result is in excellent agreement with the value predicted by *ab initio* theory. This agreement can be regarded as a significant success for the theory, since it has, in general, been difficult to predict such bond-length changes within a few tenths of a pm [7]. Looking in more detail, we note that the shrinkage is greater for removal of the $1\sigma_u$ (antibonding) electron than for removal of the $1\sigma_g$ (bonding) electron, in agreement with the weak bonding and antibonding character of these orbitals. As noted in Sec. III, the predicted value for this difference $2\delta_c$ is 0.6 pm; the values derived from the fits are somewhat less, ranging from 0.02 pm (diabatic model) to 0.29 (vibronic-coupling model).

For the changes in carbon-hydrogen bond length, the derived values are to be compared with predicted values derived from the diabatic model. The value for q_0 of zero assumed for the adiabatic fit can be ignored. We find essential agreement between the results of the fitting procedures and the theoretical predictions: q_0 is about 3 pm and δ_g is small—of order 1 pm or less. The agreement between the value of $q_0 = 2.9$ pm, derived from the experiment using the vibronic-coupling model, and the identical value predicted by *ab initio* theory is remarkable.

Turning to the force constants (Table III) and frequencies (Table IV) derived from the fits, we note that the values obtained are reasonable. The average force constant for carbon-carbon bond stretching, about 18 aJ Å^{-2}, is slightly higher than that for ethyne in its ground electronic state (15.72 and 15.85 aJ Å^{-2} for HCCH and DCCD) [24]. The *ab initio* result for this force constant, about 20 aJ Å^{-2}, is slightly higher than the values from the fits. The force con-

stant for carbon-hydrogen stretching, 6.2 to 6.6 aJ Å^{-2}, is higher than for neutral ethyne (5.92 and 5.99 aJ Å^{-2}), and is in good agreement with the theoretical values, 5.8 to 6.3 aJ Å^{-2}. In keeping with the higher force constants, the carbon-carbon and carbon-hydrogen frequencies for the core-ionized molecule are higher than those for the neutral molecule [11].

Although the increases in force constants and frequencies are consistent with the bond shrinkage that accompanies core ionization, the relative values for the carbon-carbon bond are at first glance surprising, in that the force constant for $^2\Sigma_g$ is greater than that for $^2\Sigma_u$. While one might have expected the reverse from the bonding properties of the core orbitals, this finding is, in fact, in agreement with the vibronic-coupling theory, which predicts the effect observed. Looking in detail, we note from Sec. III that the force constant is given by the expression $f_{c\pm}=f_c+6f_{ccc}\delta_{c\pm}\pm\beta_{cc}$. Recalling that $\delta_{c\pm}\approx\mp\beta_c/f_c$, we have $f_{c\pm}\approx f_c\mp(6\beta_c f_{ccc}/f_c-\beta_{cc})$. In this expression, β_c and f_{ccc} are both negative, and f_c and β_{cc} are both positive. As a result, the second and third terms are of opposite sign, and, therefore, the sign of the change in force constant depends on which dominates. In this case, this is the third term. From the fits to the data, the difference in force constants is between 0.9 and 1.7 aJ Å^{-2}, whereas the predicted value is only 0.2 aJ Å^{-2}. For the bond-length difference the theoretical value is greater than that derived from the data, and for the force-constant difference the theoretical value is less. The theoretical values of both of these depend on β_c; if the calculated value of this is too large by a factor of 2 or more, then the discrepancies between theory and experiment can be accounted for.

B. $^2\Sigma_g-^2\Sigma_u$ splitting and intensity ratio

A value of 101.6 ± 0.8 meV has been obtained for the $^2\Sigma_g-^2\Sigma_u$ ($v=0$) separation. The uncertainty is the convolution of the statistical uncertainty from the fit, plus 0.5 meV for the uncertainty in the energy scale, and 0.5 meV reflecting the range of values obtained from the different fitting models. The value of 101.6 differs slightly from the value of 105 ± 10 meV given by Kempgens *et al.* [10]. Although our value is well within the uncertainty that they have assigned to their result, there is a difference between the two procedures that leads to a difference in the direction seen here. In the fit, we have allowed for different carbon-carbon force constants for the $^2\Sigma_u$ and $^2\Sigma_g$ states and find that this leads to a higher frequency in $^2\Sigma_g$ than for $^2\Sigma_u$, by about 7 meV for HCCH and 4 meV for DCCD. Thus, the apparent $^2\Sigma_g-^2\Sigma_u$ splitting increases with vibrational quantum number and a fit that treats this as a constant will yield a greater number than one that allows for the possibility that the two vibrational frequencies are different. In fits where we have assumed the same vibrational profile for $^2\Sigma_u$ as for $^2\Sigma_g$, we obtain a $^2\Sigma_g-^2\Sigma_u$ splitting in good agreement with the value given by Kempgens *et al.*

The *ungerade/gerade* intensity ratio, 0.726 ± 0.011, represents the ratio of the intensity populating all states of the ion with overall *u* symmetry to the intensity for states with overall *g* symmetry. The uncertainty is the statistical uncertainty given by the fitting procedure convoluted with an approximately equal amount reflecting different results from different fitting models. The value of 0.726 is in essential agreement with the values of 0.71 (HCCH) and 0.74 (DCCD) that we have previously reported for excitation at a photon energy of 330 eV [12]. However, in our earlier paper we reported only the ratio for the $v=0$ intensities, whereas here we give the intensity ratio for the entire vibrational profile.

C. Linewidth

The intrinsic, or Lorentzian, linewidth reflects the rate at which the core-ionized molecule deexcites, primarily by Auger decay. The value we have found is 106 ± 2 meV, with the uncertainty estimated. This value is significantly larger than the value of 90 ± 10 meV reported by Kempgens *et al.* [10]. The magnitude of the discrepancy here is comparable to that between our result for CO_2 (98 ± 2 meV) [14] and that reported by Kivimäki *et al.* [8,25] of 78 ± 15 meV. The source of this disagreement is not known.

The linewidth for ethyne is 11 meV greater than the value we have found for methane [13]. Calculations of these linewidths based on the one-center model of Auger decay indicate either that there should be no difference between the two molecules [26] or that the width for ethyne should be about 6 meV less than that for methane [27]. On the other hand, the calculations of Hartmann indicate that the width for ethyne should be 17 meV greater than that for methane [28].

VII. CONCLUSION

The vibrational excitation that accompanies core ionization in such symmetric molecules as CH_3CH_3, CH_2CH_2, $CO_2(O\,1s)$, and $CS_2(S\,2p)$ can be accounted for with a model in which the core hole is taken to be localized on one of the equivalent atoms [4–7]. Such a model works because the splitting between the $^2\Sigma_u$ and $^2\Sigma_g$ core-hole states is small in these molecules, and, therefore, the motion follows the diabatic potential characteristic of a localized hole. This description does not work, however, for the carbon 1*s* ionization of HCCH and DCCD, where the splitting between $^2\Sigma_u$ and $^2\Sigma_g$ is about 100 meV. At the other extreme, the spectra are also not well described by a simple delocalized model in which it is assumed that the motion follows the adiabatic potentials, as would be the case if the splitting between $^2\Sigma_u$ and $^2\Sigma_g$ were very large.

To account for the observed spectra, it is necessary to take into account the coupling between the vibronic levels of the two electronic states. Of particular importance is that between the $^2\Sigma_u, v=1$ state of the antisymmetric carbon-hydrogen stretching mode and $^2\Sigma_g, v=0$ state of this mode. This coupling leads to population of the $^2\Sigma_u, v=1$ state that would not be expected in an uncoupled, delocalized picture. Taking this coupling into account leads to a fitting model that agrees well with the observed spectra. The molecular parameters—force constants and changes in bond lengths—determined in the fit are in excellent agreement with the predictions of *ab initio* theory.

ACKNOWLEDGMENTS

We are pleased to thank Lorenz Cederbaum for helpful comments. T.X.C. and T.D.T. acknowledge support from the National Science Foundation under Grant No. CHE-9727471. E.K. N.B. and J.D.B. acknowledge support from the Divisions of Chemical and Material Sciences, Office of Energy Research, U.S. Department of Energy. L.J.S. and K.J.B. thank the Research Council of Norway (NFR) for support.

APPENDIX: COMPUTATIONAL PROCEDURES

The MOLCAS [29] set of quantum chemistry programs was used throughout this paper, with molecular geometries optimized based on energy evaluations only [30]. High-level *ab initio* calculations were carried out in terms of extensive atom-centered Gaussian basis sets. Carbon was described by the completely decontracted *cc-p*VTZ set [31], augmented by tight polarization functions $(1p,2d,2f)$ as suggested by Martin and Taylor [32]. It was used together with the *cc-p*VTZ set for hydrogen.

Cubic potential energy surfaces were determined for neutral ethyne and ethyne with a localized core hole using the multireference average coupled-pair functional (MR-ACPF) method [33]. This constitutes a level of theory that is capable of recovering a large fraction of the static and dynamic correlation energy in these systems. The reference states were obtained in the complete active space self-consistent field (CASSCF) approximation, with four electrons distributed over the bonding and antibonding valence π orbitals. The variational optimization of hole states was carried out as described by Karlsen and Bø rve [34]. All configurations receiving a coefficient greater or equal to 0.05 were included as reference states in the subsequent MR-ACPF calculation, in which all valence electrons were correlated. Effects of core-valence correlation on the molecular geometries were examined in the single-reference modified CPF approximation [35]. The resulting corrections are added to the valence-correlated MR-ACPF geometries in various tables.

The CASSCF wave functions were also used to evaluate electronic coupling integrals between states having the core hole localized at different atoms, by means of the RASSI module in MOLCAS. In a basis of symmetrically orthogonalized diabatic states, the coupling integral was computed as $\beta \equiv H_{LR} - S_{LR}(H_{LL}+H_{RR})/2$, where S and H denote overlap and energy integrals in the weakly nonorthogonal basis of left and right hole states, respectively. For the geometries of interest here, the magnitude of the overlap integral is 10^{-3} a.u. or less.

[1] P. S. Bagus and H. F. Schaefer III, J. Chem. Phys. **56**, 224 (1972).
[2] A. Denis, J. Langlet, and J.-P. Malrieu, Theor. Chim. Acta **38**, 49 (1975).
[3] For a general discussion of hole localization and symmetry breaking, see R. Broer and W. C. Nieuwpoort, J. Mol. Struct.: THEOCHEM **458**, 19 (1999).
[4] M. R. F. Siggel, C. Field, L. J. Sæthre, K. J. Børve, and T. D. Thomas, J. Chem. Phys. **105**, 9035 (1996).
[5] J. Bozek, T. X. Carroll, J. Hahne, L. J. Sæthre, J. True, and T. D. Thomas, Phys. Rev. A **57**, 157 (1998).
[6] J. A. Hahne, T. X. Carroll, and T. D. Thomas, Phys. Rev. A **57**, 4971 (1998).
[7] T. D. Thomas, L. J. Sæthre, S. L. Sorensen, and S. Svensson, J. Chem. Phys. **109**, 1041 (1998).
[8] A. Kivimäki, B. Kempgens, K. Maier, H. M. Köppe, M. N. Piancastelli, M. Neeb, and A. M. Bradshaw, Phys. Rev. Lett. **79**, 998 (1997).
[9] W. Domcke and L. S. Cederbaum, Chem. Phys. **25**, 189 (1977).
[10] B. Kempgens, H. Köppel, A. Kivimäki, M. Neeb, L. S. Cederbaum, and A. M. Bradshaw, Phys. Rev. Lett. **79**, 3617 (1997).
[11] T. Shimanouchi, *Tables of Molecular Vibrational Frequencies*, Consolidated Vol. I, NSRDS-NBS, Vol. 39 (U.S. GPO, Washington, DC, 1972); NIST Chemistry Webbook, http://webbook.nist.gov/chemistry/
[12] T. D. Thomas, N. Berrah, J. Bozek, T. X. Carroll, J. Hahne, T. Karlsen, E. Kukk, and L. J. Sæthre, Phys. Rev. Lett. **82**, 1120 (1999).
[13] T. X. Carroll, N. Berrah, J. Bozek, J. Hahne, E. Kukk, L. J. Sæthre, and T. D. Thomas, Phys. Rev. A **59**, 3386 (1999).
[14] T. X. Carroll, J. Hahne, T. D. Thomas, L. J. Sæthre, N. Berrah, J. Bozek, and E. Kukk, Phys. Rev. A **61**, 042503 (2000).
[15] N. Berrah, B. Langer, A. A. Wills, E. Kukk, J. D. Bozek, A. Farhat, and T. W. Gorczyca, J. Electron Spectrosc. Relat. Phenom. **101-103**, 1 (1999).
[16] R. G. Cavell, J. Electron Spectrosc. Relat. Phenom. **6**, 281 (1975).
[17] M. Tronc, G. C. King, and F. H. Read, J. Phys. B **12**, 137 (1979).
[18] G. Strey and I. M. Mills, J. Mol. Spectrosc. **59**, 103 (1976).
[19] M. J. Bramley, S. Carter, N. C. Handy, and I. M. Mills, J. Mol. Spectrosc. **157**, 301 (1993).
[20] H. Köppel, W. Domcke, and L. S. Cederbaum, Adv. Chem. Phys. **57**, 59 (1984).
[21] P. van der Straten, R. Morgenstern, and A. Niehaus, Z. Phys. D: At., Mol. Clusters **8**, 35 (1988).
[22] K. J. Bø rve, L. J. Sæthre, J. D. Bozek, J. True, and T. D. Thomas, J. Chem. Phys. **111**, 4472 (1999).
[23] A consequence of this model is that a state that is actually of overall *g* symmetry ($v=1$, $^2\Sigma_u$) is counted as if it has *u* symmetry ($v=2$, $^2\Sigma_u$). As a result, the *ungerade/gerade* ratio from this fit is higher than obtained in the other fits.
[24] G. Herzberg, *Molecular Spectra and Molecular Structure, II, Infrared and Raman Spectra of Polyatomic Molecules* (Van Nostrand Reinhold, New York, 1945), p. 189.
[25] M. Neeb, B. Kempgens, A. Kivimäki, H. M. Köppe, K. Maier, U. Hergenhahn, M. N. Piancastelli, A. Rüdel, and A. M. Bradshaw, J. Electron Spectrosc. Relat. Phenom. **88-91**, 19 (1998).

[26] M. Coville and T. D. Thomas, Phys. Rev. A **43**, 6053 (1991).
[27] F. P. Larkins, Aust. J. Phys. **49**, 457 (1996).
[28] E. Hartmann, J. Phys. B **21**, 1173 (1988).
[29] K. Andersson, M. R. A. Blomberg, M. P. Fülscher, G. Karlström, R. Lindh, P.-Å. Malmqvist, P. Neogrády, J. Olsen, B. O. Roos, A. J. Sadlej, M. Schütz, L. Seijo, L. Serrano-Andrés, P. E. M. Siegbahn, and P.-O. Widmark, MOLCAS 4 (Lund University, Lund, Sweden, 1997).
[30] K. J. Børve, M. A. Sierka, and K. Todnem, MOLOPT (University of Bergen, Norway, Bergen, 1995).
[31] T. H. Dunning, Jr., J. Chem. Phys. **90**, 1007 (1989).
[32] J. M. L. Martin and P. R. Taylor, Chem. Phys. Lett. **225**, 473 (1994).
[33] R. J. Gdanitz and R. Ahlrichs, Chem. Phys. Lett. **143**, 413 (1988).
[34] T. Karlsen and K. J. Børve, J. Chem. Phys. **112**, 7979 (2000).
[35] D. P. Chong and S. R. Langhoff, J. Chem. Phys. **84**, 5606 (1986).